
Article

Investigation of High Vibration Phenomena in Steam Turbine: An Experimental Exploration into Root Causes and Material Analysis

Zeshan Ali ¹, Zulkarnain Abbas ^{1,*} and Saqlain Abbas ^{2,*}

¹ Department of Mechanical Engineering, National Fertilizer Corporation (NFC), Institute of Engineering and Technology, Multan 61000, Pakistan; zeshanali6007@gmail.com (Z.A.)

² Department of Mechanical Engineering, University of Engineering and Technology Lahore, Narowal Campus, Narowal 51600, Pakistan

* Corresponding author. E-mail: zulkarnain@nfciet.edu.pk (Z.A.); saqlain.abbas@uet.edu.pk (S.A.)

Received: 12 May 2024; Accepted: 11 July 2024; Available online: 15 July 2024

ABSTRACT: The steam turbine is a rotating device subject to axial and radial shaft shifts that can induce vibrations during operation. Tools such as monitoring systems and proximity probe sensors are essential to monitoring these vibrations. High vibrations affect the machine's performance, increasing the risk of malfunctions and reducing its lifespan, and also pose risks to operational and maintenance personnel. The intensified vibrations in the bearing pedestals signify the underlying issues with the machine's normal operation. Consequently, problems such as rotor imbalance, coupling misalignment, mechanical looseness, material failure, and bent shaft may be caused. In the current study, the latest field-proven automatic diagnostic of rotary equipment (ADRE 408) data acquisition system is installed by Bentley Nevada to investigate the root cause of high vibration. This advanced diagnostic system facilitates a comprehensive assessment, enabling us to effectively identify and address underlying problems. Hence, the current research includes a thorough diagnosis of the underlying problems to attenuate the risks of high vibrations in the steam turbine, coupled with strategic maintenance planning and corrective actions.

Keywords: Vibration analysis; Rotor imbalance; Material failure; Axial and radial shaft; ADRE 408



© 2024 by the authors; licensee SCIEPublish, SCISCAN co. Ltd. This article is an open access article distributed under the CC BY license (<http://creativecommons.org/licenses/by/4.0/>).

1. Introduction

Vibration, characterized by the periodic back-and-forth movement of an object, is inherent in machines due to internal and external forces. Machinery vibration encompasses the synchronized periodic motion of various components such as rotors, casing, piping, and foundation systems. The magnitude of this vibration is typically minute, requiring sophisticated equipment for detection. To provide context for the scale of machinery vibration, it can be likened to the diameter of a human hair, with an average measurement of approximately 130 μm (about 5 mil). Notably, this level of vibration is considered unacceptable for certain steam turbine generator sets, which can be as large as a house. The consequences of machine vibrations extend beyond mere movement. They induce periodic stresses in machine parts, potentially leading to fatigue failure. When the vibrational motion becomes particularly severe, it can force machine parts into unwanted contact, resulting in wear and damage. In intricate detail, machinery vibration involves the periodic oscillation of critical components [1]. Rotational components, such as rotors, and structural elements, including casings, piping, and foundation systems, all experience cyclic motion. This collective periodic motion, occurring simultaneously, highlights the dynamic nature of machinery and its susceptibility to vibrations. The significance of utilizing sensitive equipment for detection is paramount, given the typically infinitesimal scale of these vibrations.

In specific cases, such as with large steam turbine generator sets, the acceptable vibration levels are strictly regulated. Deviations beyond acceptable limits can have adverse consequences, ranging from compromised machine performance to potential structural damage. Hence, the magnitude of machine vibration involves the synchronized movement of various components, necessitating vigilant monitoring and detection due to its often imperceptible

nature. The consequences of unnoticed vibrations extend to the machine's structural integrity and operational longevity emphasizing the importance of proactive measures to mitigate potential issues [2].

Vibrations in machines induce periodic stresses in machine components, potentially leading to fatigue failure. If the vibrational motion is severe, it may cause undesirable contact between machine parts, resulting in wear or damage. Vibration analysis involves monitoring machinery's operational condition to predict potential failures and their timing. This proactive approach enables planned maintenance, allowing for replacing only those parts exhibiting signs of deterioration or damage. The fundamental principle of vibration analysis is to gather measurements that facilitate the prediction of breakdowns in specific parts and their timing. These measurements encompass machine vibration and plant operating data, such as flow, temperature, or pressure. Continuous monitoring enables the early detection of component issues, ensuring that maintenance is performed precisely when required. This approach reduces or eliminates unplanned downtime, mitigates the risk of catastrophic failure, optimizes part ordering, minimizes inventory items, and enhances efficiency by scheduling manpower effectively, consequently reducing overtime costs. The primary benefits of Predictive Maintenance (PdM) include enhanced machine reliability through effective prediction of equipment failures, reduced maintenance costs by minimizing downtime through scheduled repairs, increased production due to greater machine availability, lower energy consumption, extended bearing service life, and improved product quality [3]. Numerous components, such as bearings, gears, imbalances, etc., can cause machine vibration. Depending on the transfer function, damping, and resonances, even tiny amplitudes can significantly impact the total vibration of the machine. Every vibration source has unique frequencies that can appear as discrete frequencies, sum and/or difference frequencies, or both [4,5]. The current study will cover the investigation and diagnosis of the excessive vibration issue in the steam turbine.

De Cal and P. Fraga López (2022) [6] presented a case history addressing a steam turbine seal rub. This case history illustrates how vibration data obtained through an advanced online analysis system played a pivotal role in assessing the severity of vibrations experienced by a ship's propulsion steam turbine. While their machine plant was equipped with an advanced monitoring system, their focus on vibrations was primarily limited to an alarm system for vibration amplitude. Following a scheduled shutdown for preventive maintenance a few months after commissioning, during which the optimal conditions of the steam turbine were restored, the turbine began exhibiting brief periods of elevated vibration. Over time, these instances of high vibration became more frequent and with greater amplitude. A. Cooke, D. Roby, G. Hewitt [7] conducted a case study focusing on the detection of shaft-seal rubbing in large-scale power generation turbines using Acoustic Emission (AE). The study concluded that the high-frequency AE signatures detected at the gland/seal casings exhibited a modulation effect that proved beneficial in verifying a suspected rub. Additionally, the AE signatures revealed the possibility of two locations of rubbing, a diagnosis that might not be achievable through standard vibration analysis alone. The study presented the potential application of high-frequency AE analysis for diagnosing and verifying seal rubbing in power-generating turbine units.

The blade tip timing analysis option was also checked. The blade tip timing is not measured in this study because it is necessary to have vibration probes mounted on the casing at the blade level. However, it is essential to look into the machine's health. Blade tip timing is one of the most promising methods for determining the frequency of blade vibrations. Traditionally, strain gauges installed on the blades are used to monitor the response of rotating blades. The non-interference stress measurement system (NSMS), or blade tip timing, is a non-invasive, non-contacting substitute for strain gauges. This method measures each blade's motion using probes typically optical ones mounted on the engine housing. As a result, it is unaffected by most strain gauge drawbacks. A maximum of four probes can be considered [8–12].

Pawel Troka & Jerzy Manerowski used the nonlinear least squares Levenberg–Marquardt method in a tip-timing analysis to determine nonsynchronous multimode rotor blade vibrations, which is a novelty. This is done with two sensors in the casing and a once-per-revolution sensor. The accuracy of the nonlinear least squares Levenberg–Marquardt multimode method is compared with the one-mode linear method [13].

The current study aims to avert any catastrophic failures by analyzing the high vibration in steam turbines. Since most vibration problems occur during routine operations, this entails not only figuring out whether the machine is having problems but also identifying the specific problems or origins of the vibrations while the machine is working. Manufacturers are looking for any possible edge in today's fast-paced, cutthroat business environment to boost output, save expenses, and preserve product quality. Condition monitoring systems are required to identify machine problems and reduce unscheduled downtime and equipment breakdowns. It has been demonstrated that vibration analysis is one of the best methods for locating mechanical and electrical flaws in machines. Most vibration programs combine offline (walk around) and online monitoring. A skilled technician must walk from machine to machine for offline programs to gather vibration data.

The main objective of vibration analysis is to locate machine flaws and notify staff members that further action is required. When the required frequency of data gathering is not in line with the maintenance strategy, issues begin to arise.

2. Problem Description

Steam Turbine, which drives the Synthesis Gas Compressor, exhibited high vibration after random intervals. Norma's operating speed of the turbine is 8500–10,400 rpm. Inlet steam pressure and temperature are 114 kg/cm² and 460 °C respectively. Normal Maximum Vibration was 40 microns peak to peak at the Drive End Bearing of the HP Turbine. While after random intervals, Vibration peaks were observed till 80 micron maximum. Alarm Value was 75 microns and the Trip value was 100 microns. High vibration did not stay longer but occurred about 3 to 4 times in 24 Hours of Intervals.

The following are the main objectives of the current study;

- To investigate the root cause of high vibration by the installation of the latest field-proven automatic diagnostic of rotary equipment (ADRE 408) data acquisition system by Bentley Nevada
- To identify the probable causes of high-vibration
- To assist the maintenance team in planning in case of an emergency shutdown

3. Monitoring Tools & Experimental Setup

The monitoring system is Comprised of major 3 components

- Vibration Sensor/Proximity Probes
- Bentley Nevada 3500 System
- ADRE 408

3.1. Vibration Sensors/Proximity Probes

Vibration Sensors/ Proximity Probes are installed on the Turbine Drive and Non-Drive End Bearing sides. Two radial probes and one axial (or thrust) probe are installed on each bearing. The purpose of this triaxle probe configuration is to measure shaft vibration (and/or shaft displacement) in all three dimensions

The displacement vibration sensor, by Bently-Nevada Corporation, measures the distance between the rotating machine shaft and the probe tip using electromagnetic eddy current technology. Encapsulated wire coil powered by high-frequency alternating current (AC) makes up the sensor itself. As if the metal piece were a short-circuited secondary coil of a transformer (with the probe's coil acting as the transformer's primary winding), the magnetic field generated by the coil causes eddy currents to flow through the machine's metal shaft.

The closer the shaft moves toward the sensor tip, the tighter the magnetic coupling between the shaft and the sensor coil, and the stronger the eddy currents. The high-frequency oscillator circuit provides the sensor coil's excitation signal, which is loaded by the induced eddy currents.

Stronger eddy currents and a tighter magnetic connection between the shaft and the sensor coil occur when the shaft approaches the sensor tip. The induced eddy currents load the high-frequency oscillator circuit that supplies the excitation signal to the sensor coil. Figure 1 shows radial probe/sensor for radial vibration and axial probe/sensor for axial diaplaclemt.

The sensor coil is operated by the proximator module via a coaxial connection and is powered by an external DC power source. The proximator module outputs a DC voltage to indicate the proximity to the metal shaft; the standard calibration is 200 millivolts per mil (1 mil = 1/1000 inch) of motion. A technician adjusts the probe such that the quiescent voltage falls between the proximator's output voltage range limits.

ADRE connected to this output signal will show a direct representation of shaft vibration, as measured in the axis of the probe.

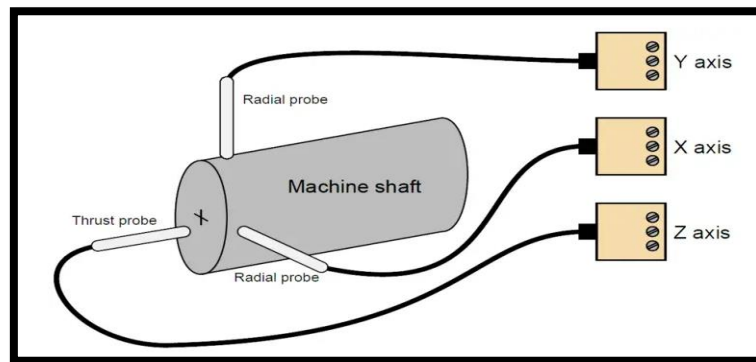


Figure 1. Working Principal of Shaft Vibration Sensor.

3.2. Bentley Nevada 3500 Series Machinery Protection System

The 3500 System offers continuous, online monitoring well-suited for machinery protection applications. It is designed to meet the criteria outlined in the American Petroleum Institute's API 670 standard for systems of this nature. The system adopts a modular rack-based design, providing a flexible and scalable approach to its configuration and implementation. The following are the key components of the equipment;

- **Transient data interface (TDI):** It serves as the primary interface for the 3500 Rack, facilitating communication with the configuration, display, and condition monitoring software. Each rack necessitates one TDI, positioned in the slot adjacent to the power supply slot. The TDI supports a proprietary protocol utilized by the 3500 Configuration Software for configuring the rack and the 3500 Operator Display Software for retrieving rack data and statuses. Moreover, the TDI offers a direct interface with the System 1 Condition Monitoring and Diagnostic software, eliminating the requirement for an external communications processor. This seamless integration enhances the efficiency of the monitoring and diagnostic processes associated with the 3500 Rack as show.
- **Relay modules:** The 3500/32M and 3500/33 Relay Modules offer a collection of relays that can be programmed to trigger based on alarm conditions detected in other monitor modules within the rack. The /32M module utilizes double-pole double-throw (DPDT) relays. In contrast, the /33 module employs single-pole double-throw (SPDT) relays. These relay modules enhance the functionality of the 3500 system by providing a configurable and adaptable means of responding to alarm conditions detected across the monitoring modules within the rack as shown in
- **Input/output (I/O) modules:** Each module within the system, including monitors, keyphrases, power supplies, communication processors, etc., necessitates a corresponding I/O (Input/Output) module. The main modules establish connections with the backplane inside the rack, and the I/O modules connect on the opposite side of the backplane, positioned behind their respective main modules. In the case of bulkhead-mounted racks only, each I/O module establishes a connection to the face of the backplane positioned above its associated main module. This configuration allows for efficient communication and data exchange between the main modules and their associated I/O modules, contributing to the overall functionality and performance of the system [14]. Figure 2 demonstrate the key components of equipment.

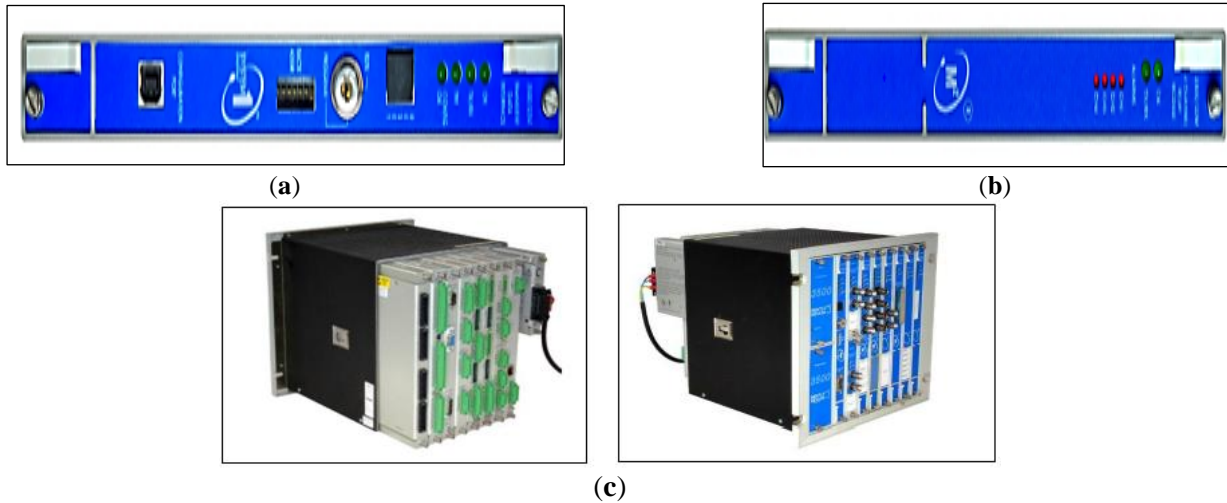


Figure 2. (a) Transient data interface (b) Relay modules (c) Input/Output Modules [14].

3.3. ADRE 408

The ADRE* Sxp Software, in conjunction with the 408 DSPI (Dynamic signal processing instrument), shown in the Figure 3, forms a highly scalable system designed for multi-channel signal processing and data acquisition. This system is tailored for real-time, highly parallel signal processing and presentation. It offers exceptional versatility by consolidating the functionality of various types of instrumentation, including oscilloscopes, spectrum analyzers, filters, signal conditioners, and digital recorders, into a unified platform.

Designed for secure corporate network environments, this system can operate remotely across a LAN/WAN or storing data independently in full “stand-alone” mode without the need for additional or external computers. Additional equipment is rarely, if ever, required. The system’s real-time display capability allows continuous data presentation independently of stored data in permanent memory.

An ADRE Sxp data acquisition system comprises:

- One or more 408 DSPI
- ADRE Sxp client software
- ADRE Quick configuration software.
- A computer system with the capability to run ADRE Sxp software.

This comprehensive setup facilitates efficient and effective multi-channel signal processing and data acquisition, making it well-suited for various applications in industrial and research environments. The 408 DSPI is a versatile instrument that offers full portability or the option to be rack-mounted, providing flexibility for operation in test stands, on-site applications, or remote locations. Its highly configurable design supports various input types, encompassing both standard and non-standard signals, including dynamic transducer signals from proximity probes, velocity transducers, and accelerometers. Each 408 DSPi unit supports up to 4 sampling cards, allowing for data acquisition from 32 channels. The base system of the 408 DSPi utilizes internal clocks and simulated speed/Keyphasor signals, supporting both asynchronous and synchronous sampling for all channels. Speed Input/Trigger cards enhance their capabilities by supporting up to 3 independent speed input channels for external speed inputs. The 408 DSPi can accommodate a maximum of 2 Speed Input/Trigger cards simultaneously, providing up to 6 physical and 6 simulated speed inputs. Users can assign any speed input (KPH) to any channel within a 408 DSPi.



Figure 3. ADRE 408 [15].

The instrument's user-friendly design enables most signal processing and sampling parameters to be modified "on the fly" without interrupting the ongoing data collection process. This feature enhances the efficiency and adaptability of the 408 DSPi for various applications in data acquisition and signal processing.

4. Research Methodology

The analysis and diagnosis of vibration issues in the steam turbine are crucial for formulating plans for ongoing maintenance and determining the necessary actions to ensure the machine's continuous, safe, and effective operation. The ADRE 408 units play a pivotal role in capturing and continuously storing data throughout the startup, operation, and shutdown phases. This continuous data acquisition simplifies the analysis of bode charts and enhances the understanding of the equipment's inherent frequencies. The insights gained from this vibration analysis not only contribute to immediate corrective actions but also inform long-term maintenance strategies and potential upgrades to optimize the performance and reliability of the steam turbine.

ISO 20816-3, titled "Mechanical vibration—Measurement and evaluation of machine vibration—Industrial machinery with a power rating above 15 kW and operating speeds between 120 r/min and 30,000 r/min", is the standard for establishing acceptable criteria for machine vibration. This document outlines general requirements for assessing the vibration of diverse industrial machines with a power rating exceeding 15 kW and operating speeds ranging from 120 r/min to 30,000 r/min when measurements are conducted in-situ. The numerical values specified in the document are intended as guidelines based on global machine experience. However, users are advised to use these values sensibly, considering specific machine features that may render the values inappropriate. Evaluating the machine condition involves considering both shaft vibration and related structural vibration, as well as specific frequency components that may not always correspond with the given broadband severity values. To facilitate this assessment, ISO categorizes machine health into different zones, with details elaborated in the standard. Table 1 classifies the machine support class, zone boundary and maximum rms vibration amplitude in both displacement and velocity units. These zones provide a structured framework for interpreting and evaluating machine vibration data to ensure effective monitoring and maintenance practices [5].

Table 1. Classification of vibration zones based on ISO 20816-3.

Support Class	Zone Boundary	r.m.s. Displacement	r.m.s. Velocity
		μm	mm/s
Rigid	A/B	29	2.3
	B/C	57	4.5
	C/D	90	7.1
Flexible	A/B	45	3.5
	B/C	90	7.1
	C/D	140	11.0

- Zone A: A freshly commissioned machine's vibration will often be found in this zone.
- Zone B: A machine is often deemed suitable for unrestricted long-term operation if its vibrations fall within this range.
- Zone C: A machine that vibrates in this area is unsuitable for continuous, long-term use.
- Zone D: Vibration levels in this area are typically considered severe enough to harm the machine.

5. Machine Description

The machine train shown in Figure 4 consists of both Low-Pressure (LP) and High-Pressure (HP) steam turbines, which drive a compressor rotating at 9000 RPM. The HP turbine is a barrel type that takes in steam at $100.7 \text{ kg/cm}^2 \text{ g}$ and is coupled to the adjacent compressor. The LP turbine, positioned externally, is a condensing type V-25, exhausting to the main vacuum condenser. Both turbines, manufactured by Siemens, are interconnected by an M.Renk solid tooth lubricated coupling. Each turbine operates at a speed of 10,000 RPM.

The steam flow from the HP turbine is divided, with a portion passing into the LP turbine and the remainder entering the Medium-Pressure (MP) steam main. The machine train has tilting pad bearings to handle radial loads and a thrust bearing to manage axial loads. Proximity vibration transducers, specifically a permanent Y & X pair, are installed on all bearings throughout the train. Additionally, thrust probes are positioned at the turbine non-drive end (NDE) to monitor axial loads. The vibration data recorded from this machine is based on shaft relative measurements.

This setup allows for comprehensive monitoring of the machine train's dynamic behavior, aiding in the early detection of potential issues and facilitating proactive maintenance to ensure the reliable and efficient operation of the steam turbines and compressor.

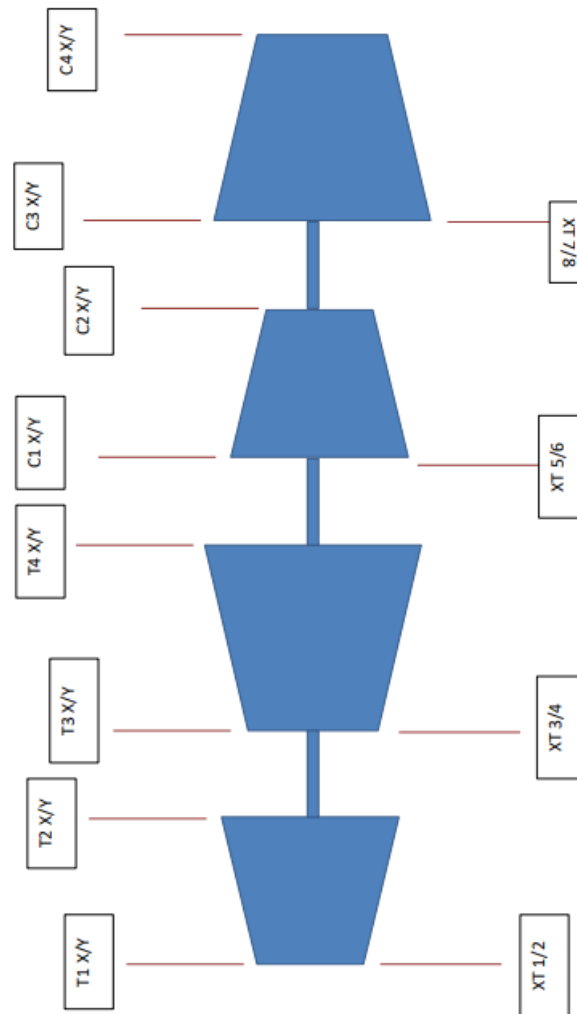


Figure 4. Machine Train.

Machine has following key components;

- Turbine case: This is a singularly crafted component, typically made from a single cast or forged steel barrel. This casing encapsulates both the bundle and rotor assembly within its structure. Integral components of the case design are the stationary and rotary blades, seamlessly incorporated as essential elements of the overall assembly [14]. Compressor casing is shown in Figure 5.
- Rotor assembly: The rotor assembly consists of a shaft onto which the balance piston, impellers, thrust bearing disc, and coupling hub (two hubs if it's a thru-drive machine) are assembled. The impellers and spacers are lightly shrink-fitted onto the shaft and keyed and secured by locknuts at each end of the assembly. The thrust disc is keyed to the shaft and is secured by a locknut. The rotor is typically driven through a gear type coupling, usually from the discharge end, although it can also be driven from the suction end.



Figure 5. Compressor and rotor casing.

- Inner oil seal: Inner oil seals are positioned in the intake and discharge heads, adjacent to the first stage inlet vane and the balance piston. These seals are specifically designed to prevent gas leakage into the bearing chambers. Figure 6a.
- Thrust bearing: The thrust bearing is of the “Michell” type, featuring several individually pivoting pads or shoes on one side of the thrust disc. Normally, rotor thrust is directed towards the intake end of the compressor. However, a thrust may occur that necessitates a double-direction thrust bearing. The bearings are supplied with lubricating oil at approximately 20 psig. Figure 6b.
- Couplings: Continuously lubricated couplings between each compressor and its corresponding driver are employed. Specifically, oil-tight coupling guards are provided, and spray tubes are utilized to direct the oil into each end of the couplings. Figure 6c.



(a)



(b)



(c)

Figure 6. (a) Oil seals (b) Turbine bearing lower half (c) Turbine coupling.

There are following issues about their impact on the vibration response of the turbine are mentioned in detail in [16–19]. The knowledge of these issues will help to understand the root causes of the vibrations.

- Eccentricity (Rotor Bow)
- Unbalance
- Misalignment
- Rubs
- Fluid-induced Instabilities
- Shaft Cracks

6. Results and Discussion

Based on operational parameters and operator feedback, all the measurements received from data acquisition are examined. The shaft vibration values retrieved from ADRE are mentioned in Table 2, and analyzed in Figure 7.

Table 2. Vibration values from ADRE.

Sr.NO	Vibration Probe Location	Channel Name	Vibration Value UP-P
1	Low-pressure turbine bearing 1, radial direction X	T1X	31.92
2	Low-pressure turbine bearing 1, radial direction Y	(T1Y)	29.35
3	Low-pressure turbine bearing 2, radial direction X	(T2X)	14.41
4	Low-pressure turbine bearing 2, radial direction Y	(T2Y)	14.02
5	High-pressure turbine bearing 3, radial direction X	(T3X)	42.37
6	High-pressure turbine bearing 3, radial direction Y	(T3Y)	40.31
7	High-pressure turbine bearing 4, radial direction X	(T4X)	62.5
8	High-pressure turbine bearing 4, radial direction Y	(T4Y)	56.02
9	Low-pressure compressor bearing 1, radial direction X	(C1X)	18.11
10	Low-pressure compressor bearing 1, radial direction Y	(C1Y)	19.59
11	Low-pressure compressor bearing 2, radial direction X	(C2X)	0.76
12	Low-pressure compressor bearing 2, radial direction Y	(C2Y)	22.69
13	High-pressure compressor bearing 3, radial direction X	(C3X)	10.01
14	High-pressure compressor bearing 3, radial direction Y	(C3Y)	43.05
15	High-pressure compressor bearing 4, radial direction X	(C4X)	0.786
16	High-pressure compressor bearing 4, radial direction Y	(C4Y)	9.83
17	Low-pressure turbine bearing 1, axial direction	(XT1)	9.17
18	Low-pressure turbine bearing 2, axial direction	(XT2)	9.94
19	High-pressure turbine bearing 3, axial direction	(XT3)	21.87
20	High-pressure turbine bearing 4, axial direction	(XT4)	22.60
21	Low-pressure compressor bearing 5, axial direction	(XT5)	37.54
22	Low-pressure compressor bearing 6, axial direction	(XT6)	37.10
23	High-pressure compressor bearing 7, axial direction	(XT7)	27.89
24	High-pressure compressor bearing 8, axial direction	(XT8)	26.44

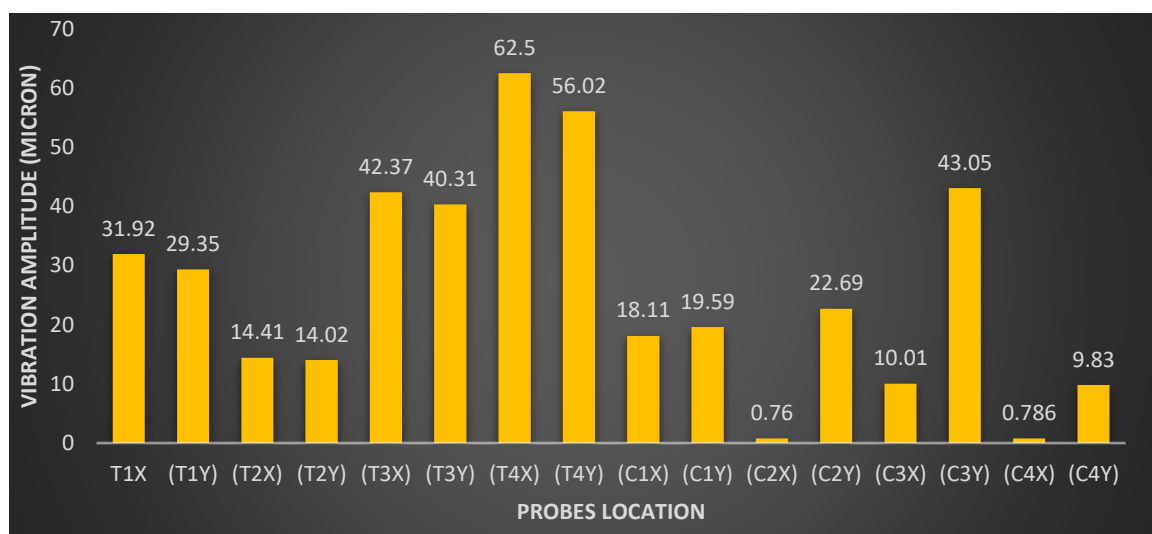


Figure 7. Analysis of vibration values.

For absolute vibration values, casing vibration data was also acquired using Portable Vibration Analyzer CSI 2140. No changing observed in casing vibration. One week of data was collected and found constant. No changes were observed in Absolute Vibration. The observations have been demonstrated in Figure 8.

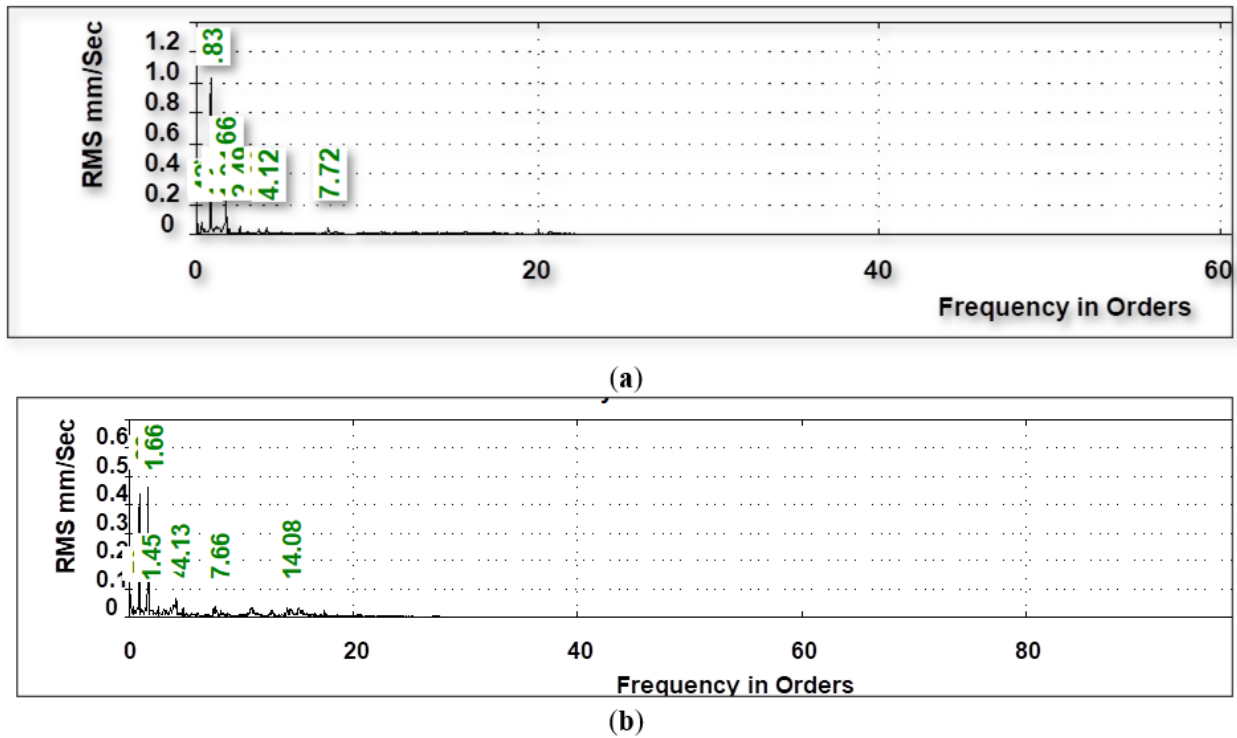


Figure 8. (a) Absolute vibration values in normal operation before high vibration (b) Absolute vibration values during high vibration.

In the next step; the shaft vibration measured data is further analyzed in different phases to demonstrate the trend, spectrum, shaft center line and orbit graphs. In the first phase, the trend plot is studied. It is a rectangular or polar plot on which the vibration value is plotted on the Y-axis and time on the X-axis as shown in Figure 9. The fluctuation in RPM is observed due to stalling at the beginning. Almost 1000 RPM fluctuations were observed in the trend plots. Further, the variations in 1X vibration & phase changes were observed in LP Turbine Drive End side Bearing T2X. In amplitude graph, the red line shows the 1X vibration and blue line represents the overall vibration value. While symbol shows that data collection was stopped at this point.

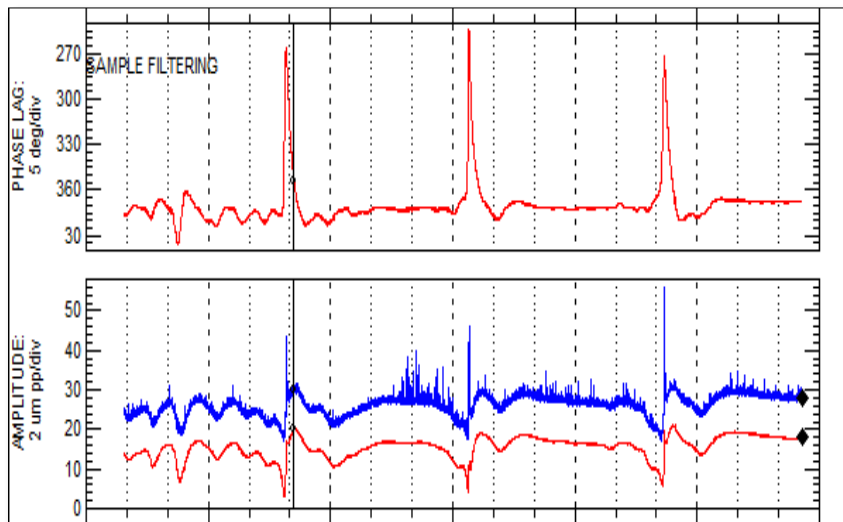


Figure 9. Trend plot (High 1X vibration and phase change).

In the second phase, the spectrum data is analyzed in Figure 10. The amplitude of vibration is plotted on the vertical axis and the vibration frequency is plotted on the horizontal axis. Sub-synchronous or sub-harmonic vibration can be observed in the HP turbine NDE Bearing T4Y spectrum. Further, the HP steam turbine orbit plot showed an elliptical shape and 2x dominant peak in the spectrum.

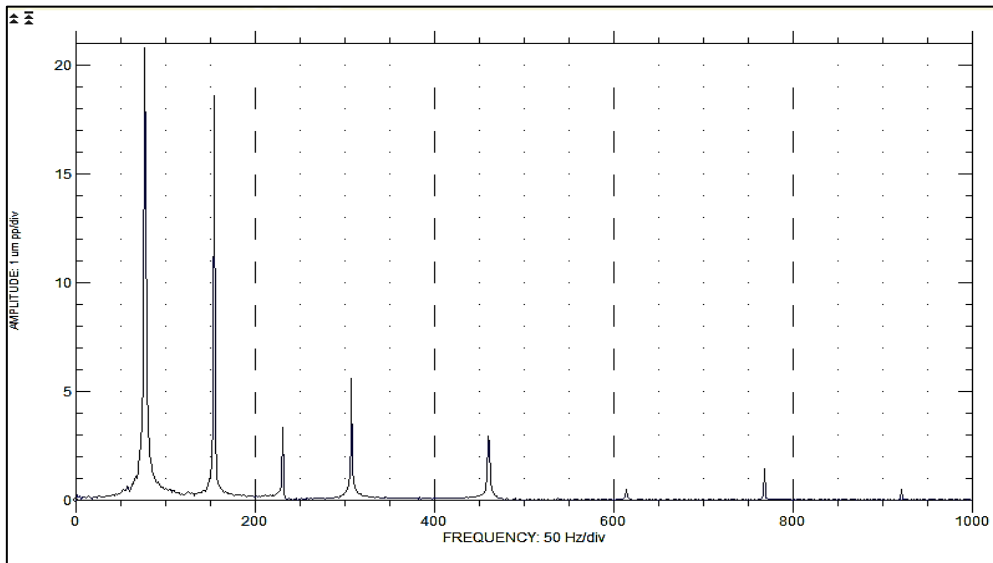


Figure 10. Spectrum plot analysis (1/2x/ sub-synchronous peak in spectrum).

In the third phase, centerline plot analysis is conducted and demonstrated in Figure 11. The shaft center line shows the shaft position in the bearing. The total lift of the shaft can also be measured from shaft center line plot analysis. The current findings show high eccentricity in the shaft centerline position of HP Turbine Bearing T4Y.

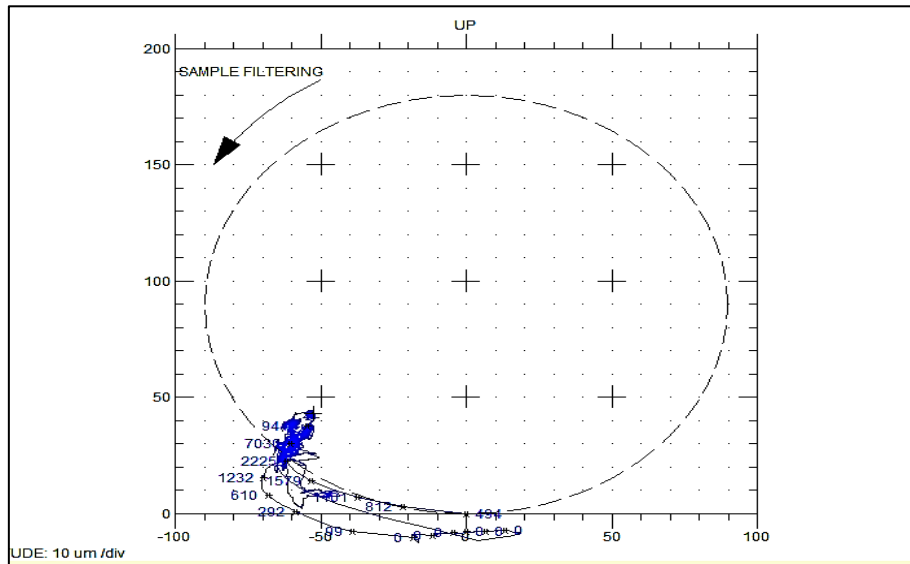


Figure 11. Centerline plot analysis.

In the last phase, orbit plot analysis is performed, as shown in Figure 12. Orbit plot displays only the dynamic motion. The purpose of the orbit plot is to show the two-dimensional complete motion of the rotor. It demonstrates the path of the rotor shaft centerline. The misalignment signs are observed during the analysis of the orbit of the machine train. Further, it is also found that there is slight ovality in the orbit.

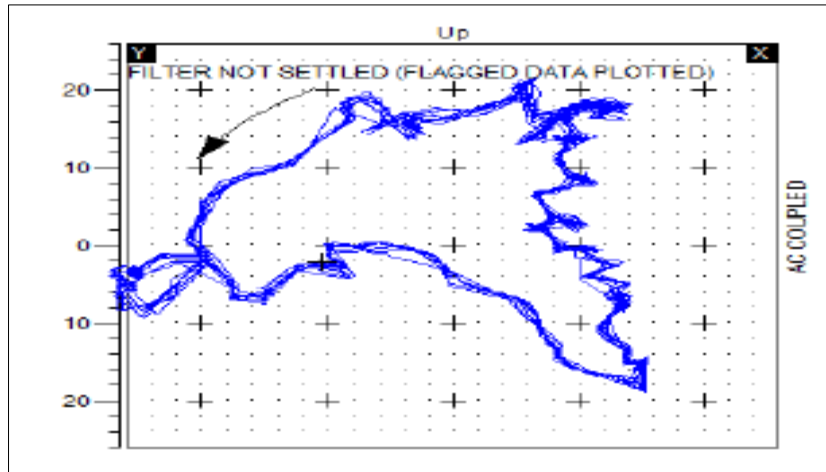


Figure 12. Orbit plot analysis.

Based on the observation mentioned above and facts, root cause analysis is performed in following sub-sections to investigate the high vibration issues.

6.1. Rotor Rub

When components within a machine shift to positions where clearances are reduced or vibrate in a manner that eliminates clearances, unintended contact can occur at locations beyond the designated bearings, resulting in what is commonly referred to as “rubbing”. During such contact events, a constraint is imposed on the motion of the rotor, introducing additional complexities. In a rubbing scenario, contact forces emerge suddenly and dissipate just as quickly. The rotor applies pressure to the stationary part while the stator exerts an equal and opposite force back against the rotor. This contact force can be broken down into tangential (frictional) and radial. The tangential friction force, as a byproduct, serves as an agent for transferring rotational energy to radial vibration. Consequently, the magnitude of vibration is prone to alteration during a rubbing event, impacting both the amplitude and phase of the vibration. Understanding these effects is crucial for monitoring and managing machine health, as rubbing can lead to wear, damage, and changes in dynamic behaviour, necessitating appropriate maintenance interventions to ensure the continued reliability of the machinery [1]. Rub symptoms and findings are described in Table 3.

Table 3. Rub symptoms and findings.

Ideal Symptoms of Rubbing	Actual Findings
Changes in 1X vibration & phase change	√
Abnormal orbit shape	√
Subsynchronous or subharmonic vibration	√
Harmonics in spectrum	√
Thermal bow	×
Change in Shaft Center Line	√
Wear, damage	×

(In Tables 3–5; √ means If symptoms found in graph. × if symptoms not found in graph).

Rubbing is consistently a secondary effect induced by various factors such as excessive radial loads, looseness, external or internal misalignment, piping strain, foundation issues, uneven thermal growth, a locked gear coupling, or a misaligned internal component. In other words, rubbing doesn’t occur in isolation but is a consequence of underlying issues that impact the proper functioning of the machinery. Excessive radial loads, whether due to imbalances or other issues, can lead to components coming into contact, resulting in rubbing. Looseness in the machinery structure or misalignments, whether internal or external, can also lead to parts shifting from their designated positions and causing unintended contact. Factors like piping strain, foundation problems, and uneven thermal growth further exacerbate the likelihood of rubbing. Even a locked gear coupling or an internal part being out of its intended position can create conditions conducive to rubbing. Figure 13 shows the rub spectrum.

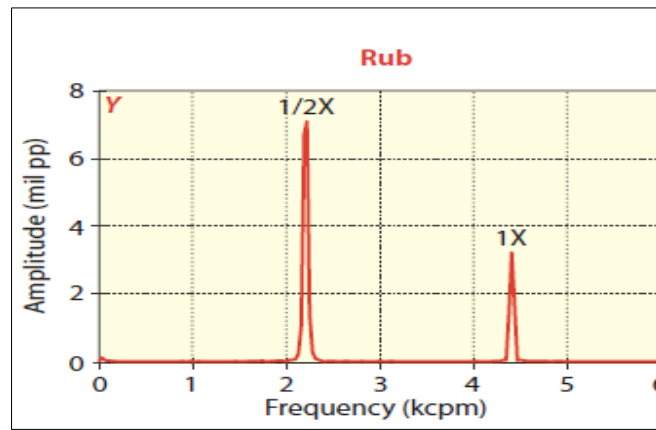


Figure 13. Rub Spectrum.

6.2. Looseness

Looseness can be attributed to worn or oversized fluid-film bearings or loose bearing support. In cases of looseness, the structural elements or bearings within the machinery experience excessive play or lack proper support. This can result in unintended movement or shifting of components, leading to vibrations with characteristic frequencies. Table 4 demonstrates the looseness symptoms and findings. While the looseness spectrum is illustrated in Figure 14.

Table 4. Looseness symptoms and findings.

Ideal Symptoms of Looseness	Actual Findings
Severe looseness will give 1/2x & 1/3x	√
Multiple peaks at running speed (up to 10x)	×
Random amplitude of waveform	×

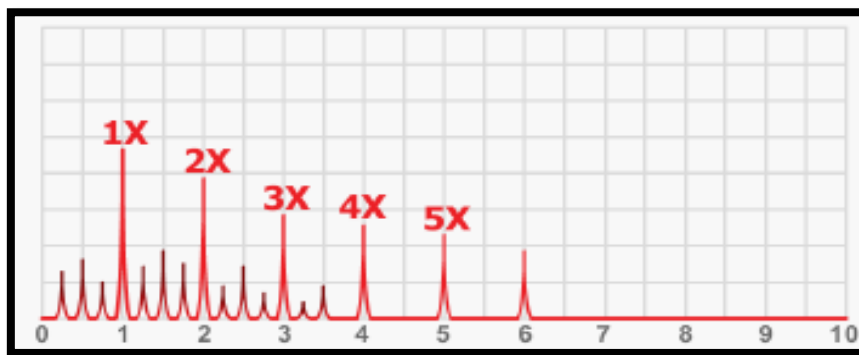


Figure 14. Looseness Spectrum.

6.3. Misalignment

In cases of misalignment, certain symptoms often occur in pairs, indicating the effects of misalignment on adjacent components. For instance, a bearing that experiences overloading due to misalignment is likely to have an underloaded neighbouring bearing. This pattern highlights the uneven distribution of forces resulting from the misalignment condition. Another misalignment indicator is the average eccentricity ratio, which can be high in one bearing and low in an adjacent bearing. This disparity in eccentricity ratios signifies the uneven distribution of loads and misalignment-induced forces across adjacent components. The shaft centerline position may also exhibit a specific quadrant in one bearing and the opposite quadrant in an adjacent bearing. This discrepancy in shaft centerline positions further underscores the impact of misalignment on neighbouring components, emphasizing the interconnected nature of symptoms associated with misalignment. The misaligned shaft has been demonstrated in Figure 15.

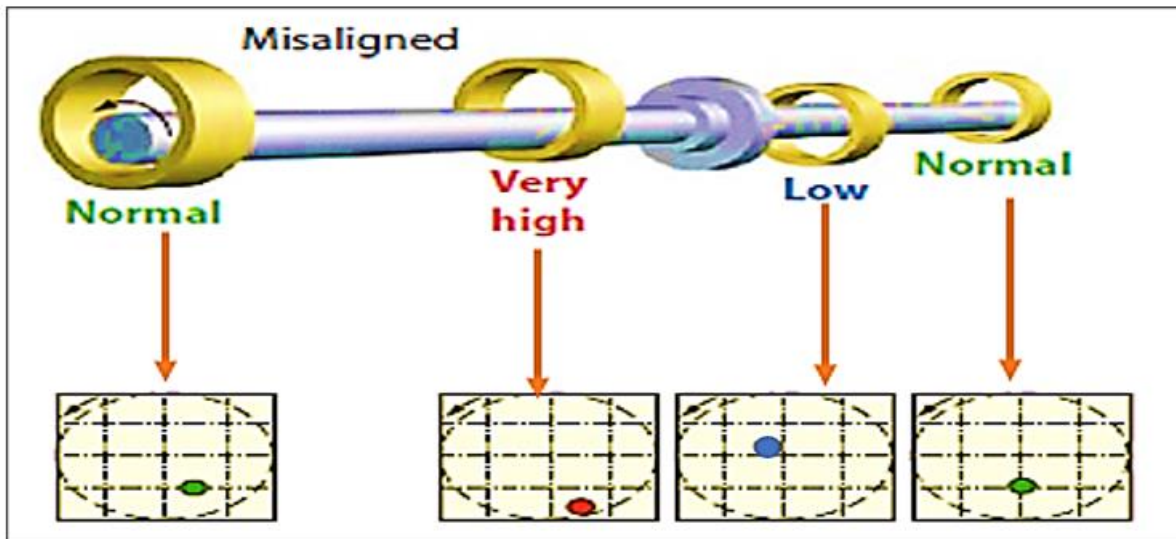


Figure 15. Misaligned shaft.

Recognizing these paired symptoms is essential for accurate diagnosis and effective corrective actions to address misalignment issues in machinery. Understanding the interrelated effects on adjacent components helps develop targeted solutions to ensure optimal machinery performance and longevity [14]. Table 5 demonstrates the misalignment symptoms and findings.

Table 5. Misalignment symptoms and findings.

Ideal Symptoms of Misalignment	Actual Findings
Abnormal orbit/Preload	√
High eccentric shaft centerline	√
1x & 2X peaks in waveform	×

7. Conclusions

In the current research, the primary causes identified for the high vibration are misalignment and high eccentricity of the shaft between the HP turbine and the LP compressor. Misalignment occurs when the shaft is not precisely straight, resulting in a deviation from its intended alignment. On the other hand, high eccentricity refers to the condition where the shaft deviates from its central axis and material failure may occur. Understanding and addressing these root causes are crucial for effective diagnosis and corrective actions. Implementing appropriate measures to realign the shaft and minimize eccentricity are essential steps in mitigating the vibration issues and ensuring the optimal performance and longevity of the machinery. Rubbing is identified as a secondary cause in this scenario. The primary contributors to the issue are misalignment and high eccentricity, which result in a heightened preload on the bearing. The increased stress on the bearing due to misalignment and high eccentricity leads to the shaft rubbing against components, making rubbing a consequential side effect of the misalignment problem.

Inspections and observations are crucial for identifying and confirming these issues. The inspection process should involve a thorough examination of the machinery, focusing on assessing the alignment and eccentricity of the shaft. Observations of the bearing conditions and any signs of rubbing, such as wear patterns or elevated temperatures, provide valuable insights into the nature and extent of the problem.

Acknowledgments

The authors would like to gratefully acknowledge the support received from the National Fertilizer Cooperation Institute of Engineering and Technology, Multan (NFC IET, Multan, Pakistan), University of Engineering & Technology Lahore to accomplish this research work.

Author Contributions

Conceptualization, Z.A. (Zeshan Ali) and S.A.; Methodology, Z.A. (Zeshan Ali); Formal Analysis, Z.A. (Zeshan Ali), Z.A. (Zulkarnain Abbas) and S.A.; Investigation, Z.A. (Zulkarnain Abbas); Resources, Z.A. (Zulkarnain Abbas); Data Curation, S.A.; Writing—Original Draft Preparation, Z.A. (Zeshan Ali); Writing—Review & Editing, Z.A. (Zulkarnain Abbas) and Z.A. (Zeshan Ali); Visualization, S.A.; Supervision, Z.A. (Zulkarnain Abbas); Project Administration, Z.A. (Zulkarnain Abbas); Funding Acquisition, Z.A. (Zulkarnain Abbas).

Ethics Statement

Not applicable.

Informed Consent Statement

Not applicable.

Funding

This research received no external funding.

Declaration of Competing Interest

The authors declare that they have no known competing financial interests or personal relationships that could have appeared to influence the work reported in this paper.

References

1. Bently DE, Hatch Charles T. Fundamentals of rotating machinery diagnostics. *Mech. Eng. -CIME* **2003**, *125*, 53–54.
2. Peng ZK, Chu FL. Application of the wavelet transform in machine condition monitoring and fault diagnostics: A review with bibliography. *Mech. Syst. Signal Process.* **2004**, *18*, 199–221.
3. Hee LM, Leong MS, Keng NW. Vibration analysis of rub in rotating machinery. *Appl. Mech. Mater.* **2013**, *390*, 215–219.
4. Rahman MF, Mehdi SN, Kumar P. Performance optimization of 500 MW steam turbine by condition monitoring technique using vibration analysis method. *Int. J. Adv. Res. Eng. Technol.* **2019**, *10*, 1–8.
5. Saraci J. The Effects of High Vibration on the Steam Turbo-Generator Machine of the Unit B1 339 MW in Thermal Power Plant “Kosovo B.” Master’s Thesis, Rochester Institute of Technology, New York, NY, USA, 2009.
6. Hahn W, Sinha JK. Vibration behaviour of a turbo-generator set. In *Vibration Engineering and Technology of Machinery: Proceedings of VETOMAC X 2014, Held at the University of Manchester, UK*; Springer International Publishing-Verlag GmbH: Heidelberg, Germany, 2015; pp. 155–161.
7. Mba D, Cooke A, Roby D, Hewitt G. Detection of shaft-seal rubbing in large-scale power generation turbines with acoustic emissions. Case study. *Proc. Inst. Mech. Eng. A J. Power Energy* **2004**, *218*, 71–81.
8. Dimitriadis G, Carrington IB, Wright JR, Cooper JE. Blade tip-timing measurement of synchronous vibration of rotating bladed assemblies. *Mech. Syst. Signal Process.* **2002**, *16*, 599–622.
9. Carrington IB, Wright JR, Cooper JE, Dimitriadis G. A comparison of blade tip timing data analysis methods. *Proc. Inst. Mech. Eng. G. J. Aerospace Eng.* **2001**, *215*, 301–312.
10. Zielinski M, Ziller G. *Optical Blade Vibration Measurement at MTU: AGARD PEP Symposium on Advanced Non-Intrusive Instrumentation for Propulsion Engines*; Ges. für Standortbetreiberdienste: Brussels, Belgium, 1997; pp. 2–24.
11. Pan M, Yang Y, Guan F, Hu H, Xu H. Sparse representation based frequency detection and uncertainty reduction in blade tip-timing measurements for multi-mode blade vibration monitoring. *Sensors* **2017**, *17*, 1745.
12. Rzadkowski R, Troka P, Manerowski J, Kubitz L, Kowalski M. Nonsynchronous rotor blade vibrations in last stage of 380 MW LP steam turbine at various condenser pressures. *Appl. Sci.* **2022**, *12*, 4884.
13. Manerowski J, Rzadkowski R, Kowalski M, Szczepanik R. Multimode tip-timing analysis of steam turbine rotor blades. *IEEE Sens. J.* **2023**, *23*, 11721–11728.
14. Sutar S, Warudkar V, Sukathankar R. Vibration analysis of rotating machines with case studies. *Int. J. Sci. Technol. Res.* **2018**, *7*, 70–76.
15. Saldivar B, Boussaada I, Mounier H, Mondié S, Niculescu SI. An overview on the modeling of oilwell drilling vibrations. *IFAC Proc. Vol.* **2014**, *47*, 5169–5174.

16. Al-Badour F, Sunar M, Cheded L. Vibration analysis of rotating machinery using time–frequency analysis and wavelet techniques. *Mech. Syst. Signal Process.* **2011**, 25, 2083–2101.
17. Bently DE, Yu JJ, Goldman P, Muszynska A. Full annular rub in mechanical seals, Part I: Experimental results. *Int. J. Rotating Mach.* **2002**, 8, 319–328.
18. Dang PV, Vo NT, Ngo TN, Le HN. Identification of unbalance in rotating machinery using vibration analyse solution. In *IOP Conference Series: Materials Science and Engineering*; IOP Publishing: Bristol, UK, 2020; p. 012011.
19. Kumar BK, Diwakar G, Satynarayana MR. Determination of unbalance in rotating machine using vibration signature analysis. *Int. J. Mod. Eng. Res.* **2012**, 2, 3415–3421.